Geomicrobiology Journal
Publication details, including instructions for authors and subscription information:
http://www.tandfonline.com/loi/ugmb20

Serpentine Dissolution in the Presence of Bacteria Bacillus mucilaginosus

Minjie Yao [a b], Bin Lian [a], H. H. Teng [c], Yangchao Tian [d] & Xiuqun Yang [a]

[a] State Key Laboratory of Environmental Geochemistry, Institute of Geochemistry, Chinese Academy of Sciences, Guiyang, China

[b] Graduate University of Chinese Academy of Sciences, Beijing, China

[c] Department of Chemistry, the George Washington University, Washington, DC, USA

[d] National Synchrotron Radiation Laboratory, University of Science and Technology of China, Hefei, China

Accepted author version posted online: 27 Apr 2012.Published online: 08 Nov 2012.

To cite this article: Minjie Yao , Bin Lian , H. H. Teng , Yangchao Tian & Xiuqun Yang (2013) Serpentine Dissolution in the Presence of Bacteria Bacillus mucilaginosus , Geomicrobiology Journal, 30:1, 72-80, DOI: 10.1080/01490451.2011.653087

To link to this article: http://dx.doi.org/10.1080/01490451.2011.653087

Geomicrobiology Journal (2013) **30**, 72–80

ISSN: 0149-0451 print / 1521-0529 online
DOI: 10.1080/01490451.2011.653087

Taylor & Francis
Taylor & Francis Group

Serpentine Dissolution in the Presence of Bacteria *Bacillus mucilaginosus*

MINJIE YAO[1,2], BIN LIAN[1]*, H. H. TENG[3], YANGCHAO TIAN[4], and XIUQUN YANG[1]

[1]*State Key Laboratory of Environmental Geochemistry, Institute of Geochemistry, Chinese Academy of Sciences, Guiyang, China*
[2]*Graduate University of Chinese Academy of Sciences, Beijing, China*
[3]*Department of Chemistry, the George Washington University, Washington, DC, USA*
[4]*National Synchrotron Radiation Laboratory, University of Science and Technology of China, Hefei, China*

Received October 2010, Accepted December 2011

Dissolution of serpentine in the presence of soil bacteria *Bacillus mucilaginosus* is examined through solution chemistry analysis, X-ray diffraction and 3D X-ray microscopy. Microbe-mineral interactions were carried out by incubating serpentine powder and the bacteria for 30 days. Measured Mg concentrations in the culture media were significantly higher than that in any of the control experiments at any time during the experiments. However, the behavior of the Mg/Si ratio was similar to what was known for inorganic dissolution of silicate minerals. XRD analysis revealed increased quantity of amorphous components in the reacted mineral samples, and tomography images showed a very porous and powdered appearance of the dissolved serpentine grains. These data suggest the dissolution probably proceeds through an incongruent route. Further, these observations imply that there is little genetic control by the microbes during the bacteria-mineral interaction; rather, the accelerated dissolution results primarily from a biologically induced process. Finally, the observed pH decrease, the presence of carboxylic acid, ketone, aldehyde, phenol, and alcohol in the metabolites suggests that organic acids and ligands secreted by the bacteria are largely responsible for the accelerated mineral dissolution.

Keywords: *Bacillus mucilaginosus*, serpentine, weathering process, mechanism, 3D image

Introduction

Weathering of serpentine rocks has received long-standing attention from soil science community because of the "serpentine syndrome" (Jenny 1980), which is characterized by plants grown from serpentine soils having (a) poor productivity, (b) high rates of endemism, and (c) vegetation types distinct from those of neighboring areas (Whittaker 1954). The interests are recently rekindled, not by the need to further probe the edaphic factors responsible for the biologically incited serpentine problems, but by the pressing issues of global warming. It was found that serpentine weathering produces soils deficient in essential plant nutrients such as K, N, and P (Brooks 1987; Proctor and Woodell 1975; Walker 1954), but rich in Mg and other biologically toxic trace elements (Alexander et al. 1989; Brady et al. 2005; Brooks 1987; Gasser and Dahlgren 1994; Schreier et al. 1987). Whereas the poor soil conditions bring forth strong chemical stress for indigenous flora and fauna, the high Mg concentration, combined with the relative fast weathering rate of serpentine, constitute a favorable scenario to sequester atmospheric CO_2.

The chemistry of serpentine weathering may be illustrated by the following reaction

$$\frac{1}{3}Mg_3Si_2O_5(OH)_4 + CO_2 = MgCO_3 + \frac{2}{3}SiO_2 + \frac{2}{3}H_2O \quad (1)$$

where serpentine is transformed into magnesite and silica. The reaction is exothermic and therefore thermodynamically favorable. The large-scale availability of serpentine and its parent minerals (olivine) as well as the stability of resultant carbonate prompted the suggestion that this reaction could potentially be an attractive option to sequester anthropogenic CO_2 (Baris et al. 2008; Huijgen and Comans 2003, 2005; Lackner et al. 1995, 1997; Seifritz 1990; Teir et al. 2009). This approach, i.e., mineral carbonation through chemical processing, can be executed *ex situ* by interacting CO_2 with high Mg silicate rocks; however, it faces stiff challenges in engineering feasibility and

This research was jointly supported by National Natural Science Foundation of China (Grant No. 40773069), National Science Foundation for Creative Research Groups (Grant No. 41021062), and Hundred Talents' Program of Chinese Academy of Sciences.

The authors are grateful to Dr. Hong Zhong of Institute of Geochemistry, Chinese Academy of Sciences for providing mineral samples, and X-ray microscope beamline U7A of National Synchrotron Radiation Laboratory, University of Science and Technology of China for three-dimensional (3D) shapes captured, and Yong Guan and Wenjie Li in there for their assistance in this work.

*Address correspondence to Bin Lian, State Key Laboratory of Environmental Geochemistry, Institute of Geochemistry, Chinese Academy of Sciences, Guiyang 550002, China; Email: bin2368@vip.163.com.

economic viability. An alternative strategy, i.e., in situ carbonate through injecting CO_2 into ultramafic rocks, may prove to be a more practical route to sequester CO_2.

In situ carbonation takes advantage of natural process of weathering and mineralization to carry out the reaction in Equation 1. The overall process of serpentine carbonation may be considered as consisting of the following two separate reactions:

$$Mg_3Si_2O_5(OH)_4 + 6H^+ = 3Mg^{2+} + 2H_4SiO_4 + H_2O \quad (2)$$

$$Mg^{2+} + CO_2 + H_2O = MgCO_3 + 2H^+ \quad (3)$$

The first reaction is silicate mineral dissolution and the second reaction carbonate crystallization. It is widely recognized that the release of Mg ions from the weathering reaction (Equation 2) is the rate-limiting step of the carbonation process in the absence of any biological activity. However, little details are known about the biological effect serpentine dissolution.

Vacha et al. (1995) showed that certain soil microorganisms accelerated the release of trace elements from serpentine as fertilizer for agricultural soils. Crawford et al. (2000) found two *Penicillium* species facilitated the degradation of serpentine. Rajkumar et al. (2009) further discussed the potential of bacteria in the phytoremediation of serpentinic soils. A recent study indicated that a rare fungal species, *Verticillium leptobactrum*, is particularly active in the bioweathering of serpentinic rocks (Daghino et al. 2009). It appears that microbial activities in natural environment may hold the key to enhance the weathering of ultramafic and serpentinic rock in the framework of carbonate sequestration.

It is well documented that bacteria can decompose silicate minerals such as mica, feldspar, quartz, kaolinite, illite, and pyroxene (Aouad et al. 2005; Bennett et al. 2001; Davis and Luttge 2005; Dong et al. 2003; Friedrich et al. 1991; Lian 1998; Liu et al. 2006; Maurice et al. 2001; Vandevivere et al. 1994). These studies suggested that different mechanisms may be operative in different scenarios. Some bacteria promote rock weathering by mobilizing mineral constituents with inorganic or organic acids or ligands that they excrete. Others promote rock weathering by redox attack of mineral constituents such as Fe and Mn (Dong et al. 2009; Ehrlich 1998). The rates of plagioclase dissolution in solutions containing organic acids are up to 10 times greater than the rates determined in solutions containing inorganic acids at the same acidity (Welch and Ullman 1993).

Microbes could make biosignatures on the surface of the weathered silicate minerals and could change their chemical components and textures by the following factors: contents of nutritious matters, organic acid, biofilm, extracellular polymeric substance and the redox reactions (Wu et al. 2007). Microbes may use organic ligands to dissolve the silicate, chelating metals, particularly Fe, for metabolic processes and also form stable complexes with Al and occasionally with Si (Rogers and Bennett 2004; Stone 1997).

Studies by Vandevivere et al. (1994) showed bacteria stimulating bytownite dissolution at near-neutral pH while in a resting state in buffered glucose, by partially oxidizing glucose to gluconate, and this gluconate-promoted dissolution was also observed with albite, quartz and kaolinite. Lian et al. (2002) proposed a comprehensive review on potassium release in studying the mechanism of silicate bacteria in releasing potassium from feldspar and illite. The mechanism about bacterial weathering of serpentine in this research may also include organic acids or ligands, extracellular polymeric substance and comprehensive mechanism, which need further study.

The goal of the present study is to examine the bioweathering process of serpentine by *Bacillus mucilaginosus*, and to evaluate which of the above-mentioned mechanisms are chiefly responsible for the microbial decomposition of serpentinic rocks.

Materials and Methods

Bacteria Cultivation

Bacteria strain (*B. mucilaginosus* K02, GenBank database accession number: HM579819, stored at Environmental Biological Science and Technology Research Center, Institute of Geochemistry, Chinese Academy of Sciences), isolated from a farmland soil in the nearby suburbs of Guiyang City, Guizhou Province, China, was identified by its morphology and 16S rDNA sequence. This kind of bacteria is a normal soil-inhabited bacteria, especially in crop soils.

The activated strain was inoculated into a 250 mL triangular flask containing 100 mL nitrogen medium (sucrose 10.0 g, yeast extract 0.3 g, $(NH_4)_2SO_4$ 0.5 g, $MgSO_4{\cdot}7H_2O$ 1.0 g, $CaCO_3$ 0.5 g, K_2HPO_4 1.0 g, distilled water 1000 mL, pH 7.0–7.5, autoclaved for 20 min at 121°C), cultured on a shaker at 28–30°C and 150 r/min for 5 days, followed by inoculated 10 mL of the activated bacterial culture in a nitrogen-free medium (sucrose 5.0 g, $MgSO_4{\cdot}7H_2O$ 0.5 g, $CaCO_3$ 0.1 g, Na_2HPO_4 2.0 g, $FeCl_3$ 0.005 g, glass dust 7.0 g, distilled water 1000 mL, pH 7.0–7.5) in a shaker at 28–30°C and 150 r/min for 5 days to enhance polysaccharide production (Chen and Lian 2005; Lian et al. 2004; Lian et al. 2008a; Mo and Lian 2011). The resultant bacterial culture was used for the serpentine weathering experiments.

Mineral Phases

The mineral assembly used in this study was serpentine rock, which contain lizardite, kaolinite, talc, nontronite and clinochlore, collected from Xingxingxia, located between Xinjiang and Gansu province of China. The chemical composition of the mineral is listed in Table 1, and the rock samples were ground and sieved to collect grains <200 mesh (approximately 75 μm).

Experimental Settings for Microbe-Mineral Interactions

One experimental run and three parallel controls were conducted to probe the bacteria-serpentine interactions. Control I (with autoclaved bacterial culture) and control II (with

Table 1. Chemical composition of the serpentine (%)

SiO_2	TiO_2	Al_2O_3	Fe_2O_3	FeO	MnO	MgO	CaO	Na_2O	K_2O	P_2O_5	LOI	Total
41.33	0.01	2.41	2.50	4.13	0.02	37.25	0.11	0.07	0.05	0.13	11.61	99.62

medium and without autoclaved bacterial culture) were identical to the experimental run (with bacterial culture), control III used deionized water instead of the culture medium, without autoclaved bacterial culture. All experiments were carried out in 250 mL triangular flasks containing 100 mL liquid medium (nitrogen-free medium with $MgSO_4 \cdot 7H_2O$ being replaced by K_2SO_4 to eliminate the effect of solution Mg^{2+} on mineral decomposition) except control III that used deionized water instead. All experiments were conducted by mixing 0.5 g of minerals into the medium, sterilizing at 121°C for 20 min. For the experimental run and control I, 5 mL of bacterial culture (the bacterial concentration in the culture was 1.8×10^9 cells/L) or autoclaved bacterial culture were inoculated into the mixture, respectively. For the control II and III, 5 mL of autoclaved medium or deionized water were inoculated into the mixture, respectively. The flasks containing the final mixtures were incubated on a shaker at 28–30°C and 150 r/min for 30 days.

The samples of the three repeats of the experimental run as well as of each of the three controls were taken out from the incubator every 5 days. Upon measuring the pH, the media were sterilized and kept static for 24 h, followed by dilution using equal (to that of the media) volume of distilled water. The diluted media were then stirred for 10 min using a magnetic stirring apparatus, heated at 80°C for 30 min in water bath, and stirred again for additional 3 min to fully disperse the bacteria-mineral complex. The samples were finally centrifuged at 5000 rpm for 10 min and the supernatant was collected to determine the quantity of dissolved magnesium and silicon. Average values (the measure value times dilution ratio) of Mg and Si contents from the three repeats were reported as the final concentrations (Lian 1998).

Sample Analysis

Magnesium and silicon contents in the growth media were analyzed by ICP-OES (Inductively Coupled Plasma Optical Emission Spectrometer, Varian, Vista MPX), and organic compositions of the metabolites by GC-MS (Gas Chromatograph-Mass Spectrometer, Waters, GC-TOF). Detailed analytical conditions of the GC-MS analysis are given as: (1) chromatographic column: DM-FFAP, 30 m × 0.25 mm, 0.25 μm; (2) carrier gas: high purity helium, 1.2 mL/min; (3) column box temperature: initial temperature was kept at 100°C for 5 min, then raised to 220°C at the rate of 10°C/min and kept for 12 min; (4) sample injection: injection port 250°C, split ratio 5:1, sample injection 1.5 μL.

Bacteria-mineral complex collected at 10 and 30 days of the experiments were oven-dried at 50°C. The powder samples were pressed and analyzed by XRD (powder X-ray diffraction, Rigaku D/Max-2200, Cu$K\alpha$ at 40 KV and 20 mA, and 3°/min scan rate) and the mineral phases were identified using the JCPDS standard (Joint Committee on Powder Diffraction Standards).

SEM (scanning electron microscopy) analysis of the bacteria-mineral complex was performed using an Amray instrument (1000 B, 15 KeV). X-ray tomography image of the reacted minerals were collected at beamline U7A of the National Synchronton Radiation Laboratory (NSRL) in Hefei, China (X-ray energy: 7 keV–11 keV, resolution: 50 nm (Rayleigh criteria), field of view: 15×15 μm^2). Sample preparation for the X-ray microscopic analysis included dispersing the complex in alcohol on a silicon nitride film fixed on the sample holder, followed by sequential image collection from $-70°$ to $+70°$ in 2° intervals at 8.0 keV. Data alignment for tomographic imaging was performed using the software provided by the Xradia Company. A standard filtered-back-projection algorithm was applied to reconstruct the aligned data.

Results

Mg, Si Released and pH Changed During Bacteria-Mineral Interactions

The amount of magnesium released in the presence of *B. mucilaginosus* at any given time in the 30-day incubation period was higher than that in any of the three control experiments (Figure 1). Rapid release of Mg was observed in the first 10 days where the Mg concentrations rose quickly from 6.5 to 37.9 mg/L. Upon reaching the maximum in day 10, dissolution seemed to reach a plateau as the Mg content in the media began to flatten out afterwards. Meanwhile, the Mg concentrations in the three control experiments showed a similar but much slower increasing trend. It appears that culture medium with autoclaved bacteria (Control I) had a noticeable effect on serpentine dissolution with the Mg concentration rose from 6.5 to 15 mg/L in the first 5 days and then flattened out after that day (see Figure 1). Little difference was seen between culture media (Control II) and deionized water (Control III) where minimal increase in Mg content was observed.

In correspondence to the Mg concentration, the Si (SiO_2) concentration ranged from 30.2 to 65.8 mg/L in the first 10 days, and then increased slowly to 78.4 mg/L in the next 20 days. For the control groups, the Si (SiO_2) concentration increased slowly with the culturing time, and showed a similar trend to that of Mg.

The range of pH change (Figure 2) in the experimental run maintained relatively small, but trended oppositely to that of Mg released, decreasing from 8.30 to 7.95 in the first 10 days before showing a slight increase afterwards. In comparison, pH change in the three control experiments was all within less than 0.1 unit, although the overall trend looked similar to that in the experimental run.

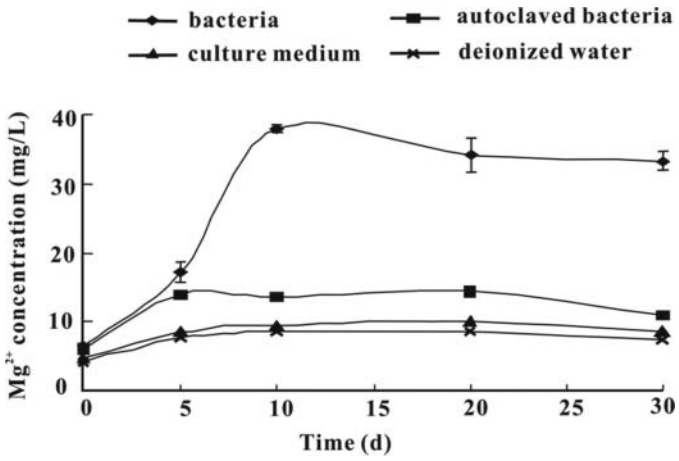

Fig. 1. Experimental measurements of Mg concentration about bacterial action samples and other three control groups during a 30-day period of incubation, the bacterial action samples released Mg rapidly in the first 10 days, upon reaching the maximum, the Mg content in the media began to flatten out afterwards. Meanwhile, the Mg concentrations in the three control experiments showed a similar but much slower increasing trend.

GC-MS Analysis of the Bacterial Metabolite

The culture media in the experimental run showed the presence of methyl butyrate, acetic acid, methyl acetate, and butyraldehyde in addition to 2-Hydroxy-gamma-butyrolactone, and 5-hydroxymethyl furancarboxaldehyde which were seen in the control I (peaks 1, 2 in Figure 3). Small amounts of several other organic compounds, such as propionic acid, benzyl alcohol, phenol, furfuryl alcohol, cyclopentanone-1, 2-dione, were also detected.

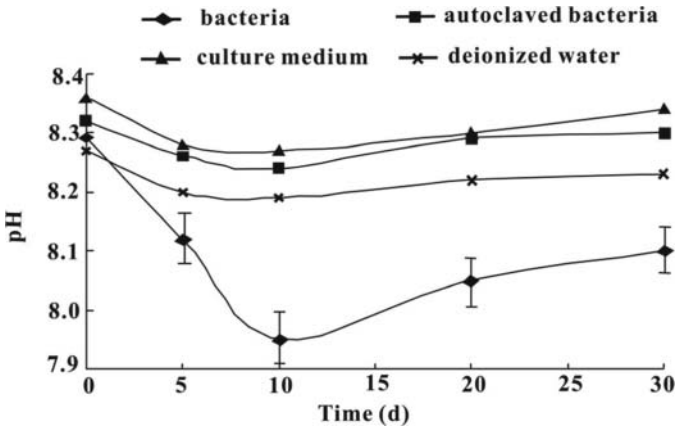

Fig. 2. Experimental measurements of pH about bacterial action samples and other three control groups during a 30-day period of incubation, the pH of bacterial action samples decreased in the first 10 days, and then showing a slight increase afterwards. In comparison, the pH changed little in the three control experiments.

Structural and Morphological Changes of Serpentine upon Bacterial Interaction

Microscopic analysis by SEM revealed the increased formation of bacteria-mineral complex over incubation time (Figure 4). The individual grains of pristine serpentine often had irregular shapes and sharp edges (Figure 4a). SEM images of the mineral samples at 10 and 30 days after incubation with the bacterial showed clumped and bio-film covered complex. It appears that the complex became more pronounced over the length of the incubation period (Figures 4b and 4c).

Compared to the pristine mineral sample, XRD analyses on the bacteria-reacted serpentine revealed an increase d-value, widened peaks (Figure 5, zone 1), weakened crystallinity (Figure 5, zone 3), as well as elevated background noise (Figure 5, zone 2). All the changes indicated an increase in the amount of amorphous components in the system. Furthermore, it appears that the structure changes became more substantial with prolonged incubation time.

Further examination of the complex by the synchrotron based transmission X-ray microscope revealed a 3-dimensional view (from two orthogonal directions, Figure 6) of the evolution of the bacteria-mineral complexes over time. Compared to the pristine serpentine (Figure 6a), the grains reacted for 30 days (Figure 6b) showed increased inter-grain spaces despite the presence of bio-film cements (Figure 4c). Up to 90 days of extended interaction rendered the dis-integration of the mineral particles (Figure 6c), as indicated by powdered appearance of the samples.

Discussion

Dissolution Stoichiometry and its Mechanistic Ramification

If proceeding through Equation 2, serpentine dissolution should yield a Mg/Si ratio of 3:2 in the effluent solutions. However, numerous previous studies have shown that silicate dissolution, particularly aluminosilicate, does not follow the stoichiometric route during the entire dissolution. Substantial amount of experimental data, either from monitoring solution composition changes during dissolution or *ex situ* examining mineral-solution interfaces, indicate the occurrence of incongruent dissolution, particularly earlier in the process, followed by a gradual transition to congruent decomposition after an extended period of reaction (Berner and Holdren Jr 1979; Casey et al. 1988, 1989; Hellmann et al. 1990; Lee and Parsons 1995; Petit et al. 1990; Petrovic 1976).

Although most of such observations were made on feldspars, ultramafic and mafic minerals do not seem to behave significantly differently as the Si-rich surface layers were frequently observed and analysed in the process of mineral dissolution. Surface analytical techniques, such as X-ray photoelectron spectroscopy (XPS), are useful tools for elucidating the mechanisms of chemical weathering. Studies on laboratory weathering of olivines have demonstrated the $SiO_2 \cdot nH_2O$ formed on the mineral surface in which Fe and Mg are depleted (Seyama et al. 1996). Zakaznova-Herzog et al. (2008) used improved XPS to investigate the surface alteration of

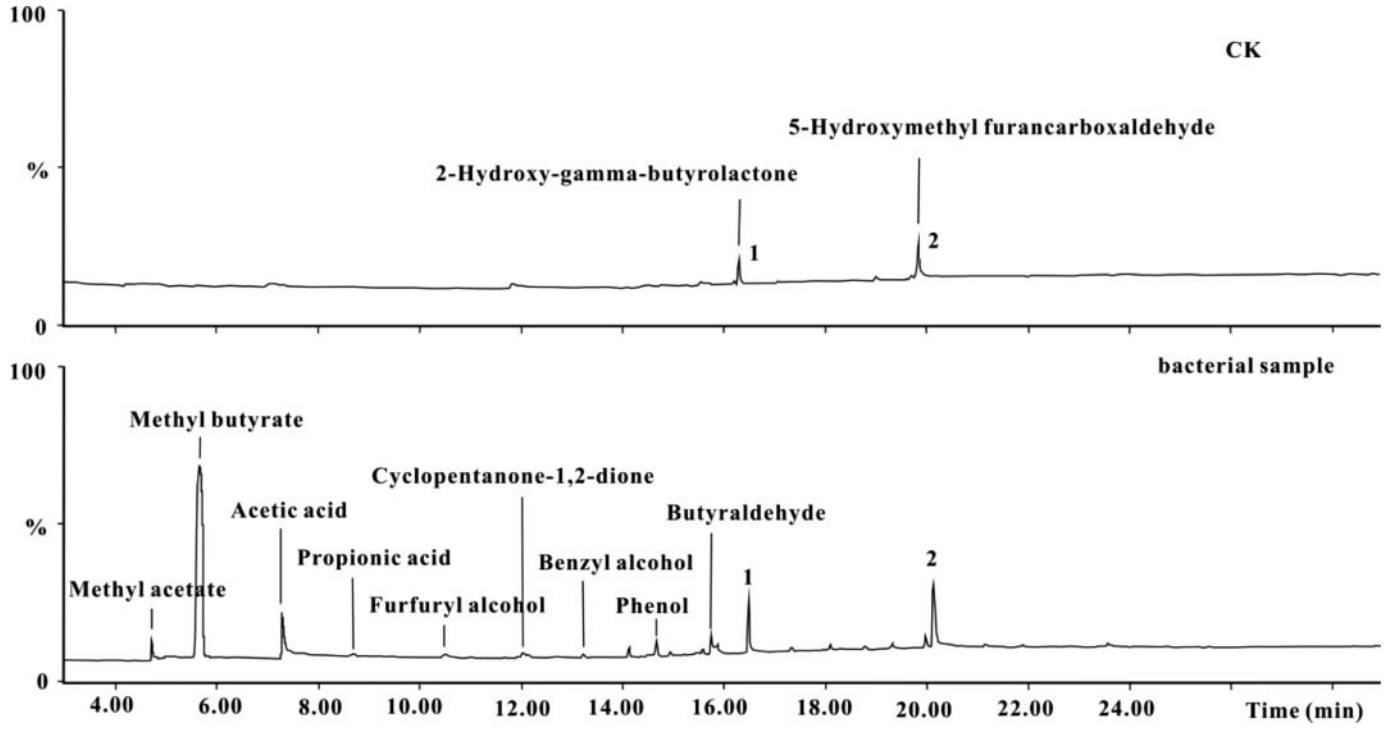

Fig. 3. GC-MS spectra of the growth media after 20 days of incubation (Top spectrum is that of the Control I with autoclaved bacterial culture), some organic compounds were detected, such as methyl butyrate, acetic acid, methyl acetate, and butyraldehyde, in addition to 2-Hydroxy-gamma-butyrolactone and 5-hydroxymethyl furancarboxaldehyde which were seen in the Control I (CK).

pyroxene, which showing the leached surfaces have monolayer OH^- coverage to give surface complexes, and the reactions are followed by a nucleophilic attack of H_2O (or H_3O^+) on Si of $H_4Si_2O_6$ (surf) and this reaction is responsible for rupture of the brigding oxygen bond of the Si–O–Si moiety and release of H_4SiO_4 to solution.

An inspection of the Mg/Si ratio in the present study (Figure 7) seems to suggest that biologically promoted serpentine dissolution largely follows the abovementioned general trend. Rapid release of Mg was observed in the very beginning (Mg/Si $\sim$ 2.75), followed by a gradual decrease of the ratio in the first 10 days, and the eventual stabilization after about 20 days at the stoichiometric value of 1.5. One of the direct implications of this similarity is that the bacteria *B. mucilaginosus* likely have promoted serpentine dissolution through a "biologically induced" rather than "biologically controlled" process (Lowenstam 1981). Measured pH changes (Figure 2) during the experiments offer additional support for this claim.

It is widely accepted that silicate dissolution starts from a very rapid exchange of surface cations for hydrogen ions followed by a much slower process of silicate framework destruction (Blum and Stillings 1995). As such, there should be a net proton change (i.e., acidity increase) in the solution. However, experimental data show a synchronous decrease of

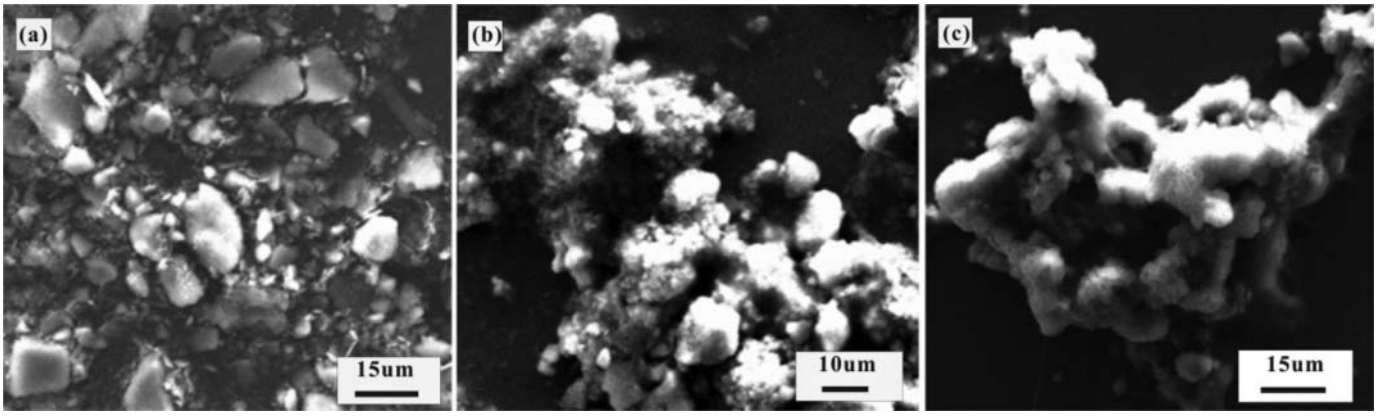

Fig. 4. SEM micrographs showing the interaction between serpentine and *Bacillus mucilaginosus* for the original sample (a), bacterially reacted samples for 10 days (b) and 30 days (c). The bacterial reacted samples occur as bacteria–mineral associations.

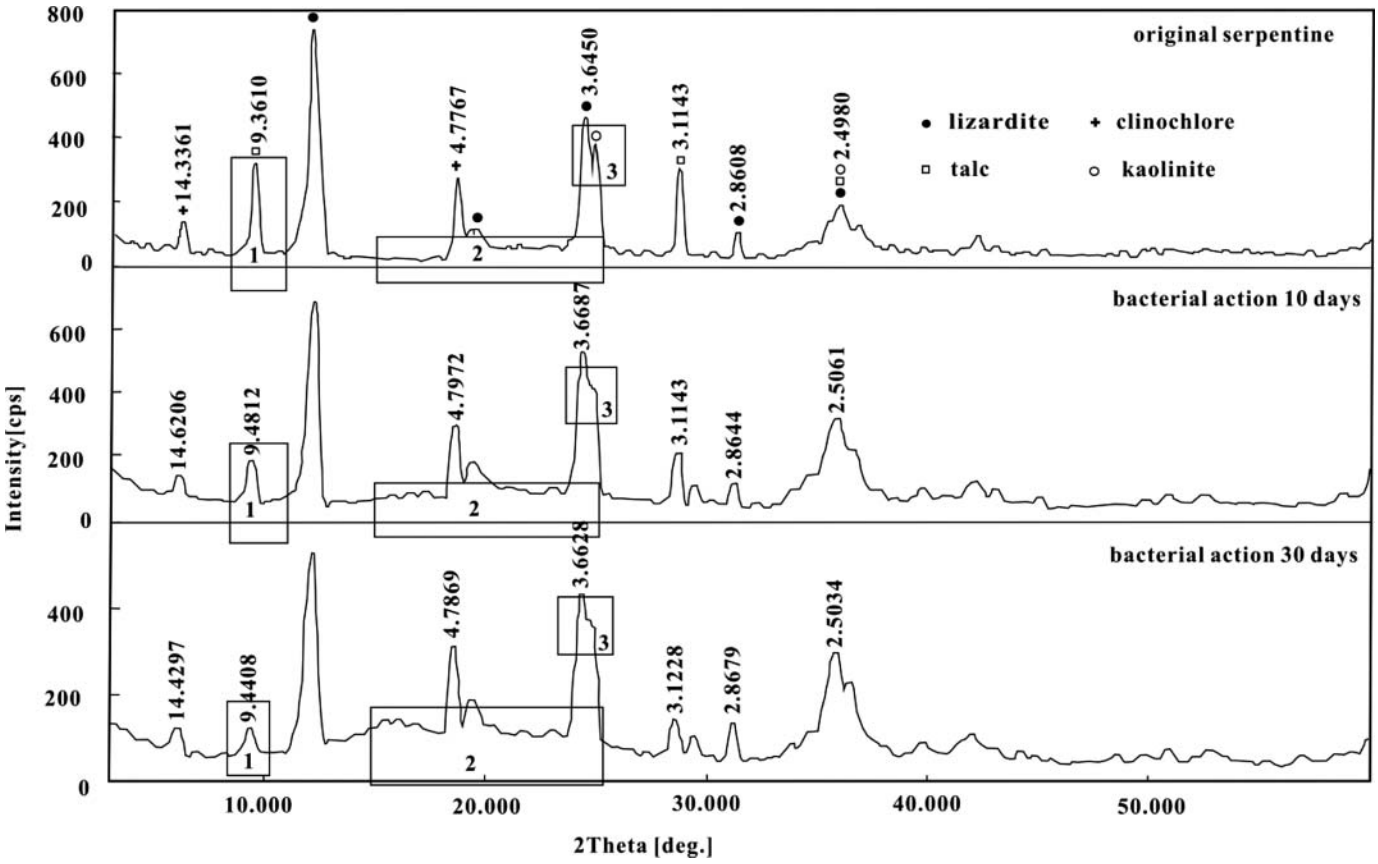

Fig. 5. X-ray diffraction (XRD) analysis of the original serpentine and the samples incubated with *Bacillus mucilaginosus* for 10 and 30 days. The samples are expressed in terms of changes of d-value, peak sharpness and width (1), background value (2) and crystallinity (3). The d-value increased, peak sharpness lost, peak width and background value increased, crystallinity decreased compared to the original serpentine, and the changes were growing with prolonged incubation time.

pH during the fast release of Mg, suggesting that the rapid dissolution in the first few days is facilitated by the organic acid associated with the initial cell growth. The quick increase of acetic acid (Figure 8) in the first 10 days demonstrates the availability of protons during this period of growth.

On a related note, if the initial fast dissolution is the work of a genetically controlled process, we would expect the Mg/Si ratio to stop the decrease once it reaches a stationary phase for the bacterial growth and then maintains at that level for a period of time. The fact that it quickly reversed, despite the still increasing (albeit slower) concentration of acetic acid, suggests that the dissolution is likely reached a stage where the residual amorphous Si-rich surface layers has built up enough thickness to slow down the Mg release process (Casey et al. 1989). Finally after about 20 days, the rate of Mg release from serpentine and that of Si release from the Si-rich surface layer reached a steady state, leading to the Mg/Si ratio close to its theoretical value of 3:2. The loss of crystallinity in the serpentine sample after bacterial interaction (Figure 5) provides proof for the increased content of amorphous material in the reaction system.

X-ray tomographic images further confirm the incongruent nature of the bacteria-serpentine reaction (Figure 6). If the release of Mg and Si follows the stoichiometric path, we would expect to see mineral grains decreasing their sizes over time but maintaining the solidity. The sponge-like appearances of the reacted mineral samples do not corroborate such hypothesis. Rather, they suggest a preferential release of certain mineral components and a gradual disruption of the silicate framework afterwards.

Role of Organic Ligands During Serpentine Dissolution

Although the initial fast release of Mg in our study may be attributed to the pH effect, it is important to realize that the overall pH change (Figure 2) is rather limited with a maximal decrease of ~0.4 unit. Hence, it is plausible to suggest that other factor may have played an important role in the increase of Mg concentration (up to ~ 4 times, Figure 1) in the bacterial media relative to that in the control experiments. GC-MS analyses of the bacterial media (Figure 3) indeed found the presence of organic compounds other than acid. These organic molecules can act as organic ligands to form surface or aqueous complexes to further facilitate the dissolution reaction (Adamo and Violante 2000; Barker et al. 1997; Rogers and Bennett 2004).

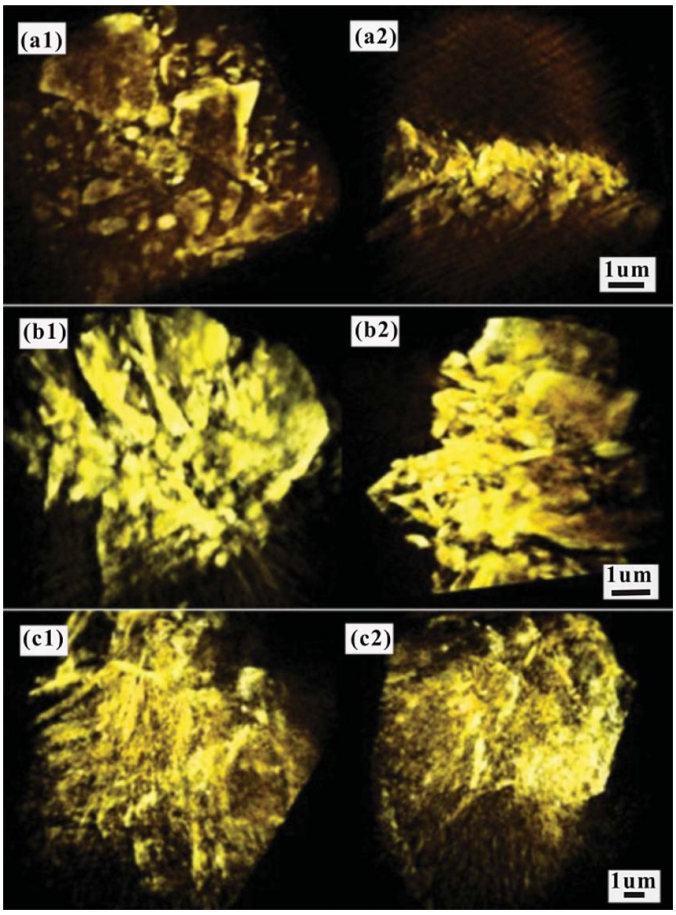

Fig. 6. 3D rendering showing the interaction between serpentine and *Bacillus mucilaginosus* for the original samples (a), bacterially reacted samples for 30 days (b) and 90 days (c). Images 1 and 2 were viewed samples in different by orthogonal angles. Notice the powdered vs granular appearance of the samples in (c) and (a) (color figure available online).

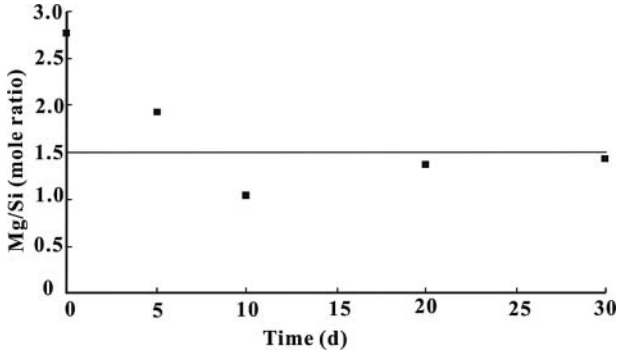

Fig. 7. Analysis of Mg/Si mole ratio about bacterial action samples during a 30-day period of incubation. The Mg/Si ratio decreased gradually in the first 10 days, and reached the eventual stabilization after about 20 days at the stoichiometric value of 1.5.

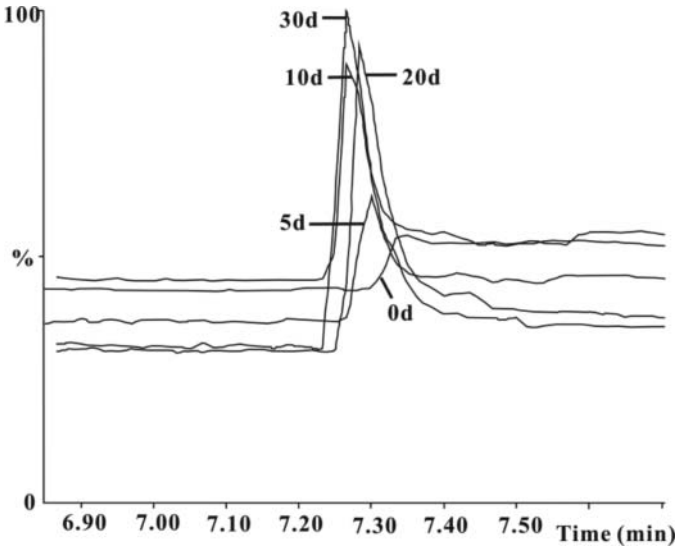

Fig. 8. GC-MS spectra of organic matters showing the changes of acetic acid peak about bacterially reacted samples after 0, 5, 10, 20 and 30 days of incubation. The acetic acid increased quickly in the first 10 days, and then changed little afterwards.

For example, the formation of surface complexes between ions on serpentine and organic ligand in the media can weaken the chemical bonds in the bulk minerals and lead to an accelerated elemental release (Banfield et al. 1999; Ehrlich 1998; Harley and Gilkes 2000; Lian et al. 2008b; Welch et al. 2002; Yao and Lian 2011). Aqueous complexes involving these organic ligand and Mg also have the potential to shift the dissolution equilibrium. The present study does not have provide enough information for us to quantify these complexation reactions, but the mere presence of these organic ligands in the bacterial metabolites suggest at least qualitatively that pH effect is not the only driving forces for the accelerated serpentine dissolution.

Conclusions

Examination of serpentine dissolution in the presence *B. mucilaginosus* indicates that the microbe promotes mineral dissolution. The behavior of Mg/Si ratio over time during the experiments is similar to what is known for silicate dissolution in inorganic environments, hence implicates that the microbially promoted serpentine dissolution is likely a biologically induced process. The increase of amorphous contents revealed by XRD as well as the sponge-like appearance of the reacted serpentine shown by tomographic imaging supports the occurrence of incongruent dissolution. Further analysis of the pH changes as well as the chemical makeup the bacterial metabolite suggests that organic acids and ligands secreted by the bacteria are largely responsible for the accelerated mineral dissolution.

References

Adamo P, Violante P. 2000. Weathering of rocks and neogenesis of minerals associated with lichen activity. Appl Clay Sci 16:229–256.

Alexander E, Adamson C, Zinke P, Graham R. 1989. Soils and conifer forest productivity on serpentinized peridotite of the trinity ophiolite, California. Soil Sci 148:389–465.

Aouad G, Geoffroy V, Meyer JM, Crovisier JL, Damidot D, Stille P. 2005. Definition of a growth medium to study the alteration of silicates in the presence of *Pseudomonas aeruginosa*. Comptes Rendus Geosci 337:1340–1347.

Banfield JF, Barker WW, Welch SA, Taunton A. 1999. Biological impact on mineral dissolution: Application of the lichen model to understanding mineral weathering in the rhizosphere. Proc Natl Acad Sci USA 96:3404–3411.

Baris K, Ozarslan A, Sahin N. 2008. The assessment for CO_2 sequestration potential by magnesium silicate minerals in Turkey: cases of Orhaneli-Bursa and Divrigi-Sivas regions. Energ Explor Exploit 26:293–309.

Barker WW, Welch SA, Banfield JF. 1997. Biogeochemical weathering of silicate minerals. Rev Mineral Geochem 35: 391–428.

Berner RA, Holdren Jr GR. 1979. Mechanism of feldspar weathering–II. Observations of feldspars from soils. Geochim Cosmochim Acta 43: 1173–1186.

Bennett PC, Rogers JR, Choi WJ, Hiebert FK. 2001. Silicates, silicate weathering, and microbial ecology. Geomicrobiol J 18:3–19.

Blum AE, Stillings LL. 1995. Feldspar dissolution kinetics. Rev Miner Geochem 31:291–351.

Brady KU, Kruckeberg AR, Bradshaw H. 2005. Evolutionary ecology of plant adaptation to serpentine soils. Ann Rev Ecol Evol System 36:243–266.

Brooks RR. 1987. Serpentine and its Vegetation. London and Sydney: Croom Helm. p. 18–28.

Casey WH, Westrich HR, Arnold GW. 1988. Surface chemistry of labradorite feldspar reacted with aqueous solutions at pH = 2, 3, and 12. Geochim Cosmochim Acta 52:2795–2807.

Casey WH, Westrich HR, Arnold GW. 1989. The surface chemistry of dissolving labradorite feldspar. Geochim Cosmochim Acta 53:821–832.

Chen Y, Lian B. 2005. Ability of *Bacillus mucilaginosus* GY03 strain to adsorb chromium ions. Pedosphere 15:225–231.

Crawford RH, Floyd M, Li CY. 2000. Degradation of serpentine and muscovite rock minerals and immobilization of cations by soil *Penicillium* spp. Phyton-Annales Rei Botanicae 40:315–321.

Daghino S, Turci F, Tomatis M, Girlanda M, Fubini B, Perotto S. 2009. Weathering of chrysotile asbestos by the serpentine rock-inhabiting fungus *Verticillium leptobactrum*. FEMS Microbiol Ecol 69:132–141.

Davis KJ, Luttge A. 2005. Quantifying the relationship between microbial attachment and mineral surface dynamics using vertical scanning interferometry (VSI). Amer J Sci 305:727–751.

Dong HL, Jaisi DP, Kim J, Zhang GX. 2009. Microbe-clay mineral interactions. Amer Mineral 94:1505–1519.

Dong HL, Kukkadapu RK, Fredrickson JK, Zachara JM, Kennedy DW, Kostandarithes HM. 2003. Microbial reduction of structural Fe(III) in illite and goethite. Environ Sci Technol 37:1268–1276.

Ehrlich HL. 1998. Geomicrobiology: its significance for geology. Earth-Sci Rev 45:45–60.

Friedrich S, Platonova NP, Karavaiko GI, Stichel E, Glombitza F. 1991. Chemical and microbiological solubilization of silicates. Acta Biotechnol 11:187–196.

Gasser UG, Dahlgren RA. 1994. Solid-phase speciation and surface association of metals in serpentinitic soils. Soil Sci 158:409–420.

Harley AD, Gilkes RJ. 2000. Factors influencing the release of plant nutrient elements from silicate rock powders: a geochemical overview. Nutr Cycl Agroecosys 56:11–36.

Hellmann R, Eggleston CM, Hochella Jr MF, Crerar DA. 1990. The formation of leached layers on albite surfaces during dissolution under hydrothermal conditions. Geochim Cosmochim Acta 54:1267–1281.

Huijgen W, Comans R. 2003. Carbon dioxide sequestration by mineral carbonation: Literature review. Petten: Energy Research Centre of the Netherlands (ECN). Energy Research Centre of the Netherlands, volume 3.

Huijgen W, Comans R. 2005. Carbon dioxide sequestration by mineral carbonation: Literature review update 2003–2004. Petten: Energy Research Centre of the Netherlands (ECN). Energy Research Centre of the Netherlands, volume 5.

Jenny H. 1980. The Soil Resource; Origin and Behaviour. New York: Springer-Verlag.

Lackner KS, Butt DP, Wendt CH. 1997. Progress on binding CO_2 in mineral substrates. Energy Convers Mgmt 38:S259–S264.

Lackner KS, Wendt CH, Butt DP, Joyce EL. 1995. Carbon dioxide disposal in carbonate minerals. Energy 20:1153–1170.

Lee MR, Parsons I. 1995. Microtextural controls of weathering of perthitic alkali feldspars. Geochim Cosmochim Acta 59: 4465–4488.

Lian B. 1998. A study on how silicate bacteria GY92 dissolves potassium from illite. Acta Mineral Sin 18: 234–238.

Lian B, Chen Y, Yuan S, Zhu LJ, Liu CQ. 2004. Study on the flocculability of metal ions by *Bacillus mucilaginosus* GY03 strain. Chin J Geochem 23:380–386.

Lian B, Chen Y, Zhao J, Teng HH, Zhu LJ, Yuan S. 2008a. Microbial flocculation by *Bacillus mucilaginosus*: Applications and mechanisms. Bioresour Technol 99:4825–4831.

Lian B, Fu PQ, Mo DM, Liu CQ. 2002. A comprehensive review of the mechanism of potassium releasing by silicate bacteria. Acta Mineral Sin 22:179–183.

Lian B, Wang B, Pan M, Liu C, Teng HH. 2008b. Microbial release of potassium from K-bearing minerals by thermophilic fungus *Aspergillus fumigatus*. Geochim Cosmochim Acta 72:87–98.

Liu W, Xu X, Wu X, Yang Q, Luo Y, Christie P. 2006. Decomposition of silicate minerals by *Bacillus mucilaginosus* in liquid culture. Environ Geochem Health 28:133–140.

Lowenstam HA. 1981. Minerals formed by organisms. Science 211: 1126.

Maurice PA, Vierkorn MA, Hersman LE, Fulghum JE, Ferryman A. 2001. Enhancement of kaolinite dissolution by an aerobic *Pseudomonas mendocina* bacterium. Geomicrobiol J 18:21–35.

Mo BB, Lian B. 2011. Hg (II) adsorption by *Bacillus mucilaginosus*: mechanism and equilibrium parameters. World J Microbiol Biotechnol 27:1063–1070.

Petit JC, Mea GD, Dran JC, Magonthier MC, Mando P, Paccagnella A. 1990. Hydrated-layer formation during dissolution of complex silicate glasses and minerals. Geochim Cosmochim Acta 54: 1941–1955.

Petrovic R. 1976. Rate control in feldspar dissolution–II. The protective effect of precipitates. Geochim Cosmochim Acta 40:1509–1521.

Proctor J, Woodell SRJ. 1975. The ecology of serpentine soils. Adv Ecol Res 9: 255–366.

Rajkumar M, Prasad MNV, Freitas H, Ae N. 2009. Biotechnological applications of serpentine soil bacteria for phytoremediation of trace metals. Crit Rev Biotechnol 29:120–130.

Rogers JR, Bennett PC. 2004. Mineral stimulation of subsurface microorganisms: release of limiting nutrients from silicates. Chem Geol 203:91–108.

Schreier H, Omueti J, Lavkulich L. 1987. Weathering processes of asbestos-rich serpentinitic sediments. Soil Sci Soc Am J 51:993–999.

Seifritz W. 1990. CO_2 disposal by means of silicates. Nature 345:486.

Seyama H, Soma M, Tanaka A. 1996. Surface characterization of acid-leached olivines by X-ray photoelectron spectroscopy. Chem Geol 129:209–216.

Stone AT. 1997. Reactions of extracellular organic ligands with dissolved metal ions and mineral surfaces. Geomicrobiol: Interact Microbes Min 35: 309–344.

Teir S, Eloneva S, Fogelholm CJ, Zevenhoven R. 2009. Fixation of carbon dioxide by producing hydromagnesite from serpentinite. Appl Energ 86: 214–218.

Vacha R, Podlesakova E, Nemecek J. 1995. The use of crushed serpentine alternative fertilizer. Rost Vyroba 41:459–462.

Vandevivere P, Welch SA, Ullman WJ, Kirchman DL. 1994. Enhanced dissolution of silicate minerals by bacteria at near-neutral pH. Microb Ecol 27:241–251.

Walker RB. 1954. The ecology of serpentine soils. II. Factors affecting plant growth on serpentine soils. Ecology 35:259–266.

Welch SA, Taunton AE, Banfield JF. 2002. Effect of microorganisms and microbial metabolites on apatite dissolution. Geomicrobiol J 19:343–367.

Welch SA, Ullman WJ. 1993. The effect of organic-acids on plagioclase dissolution rates and stoichiometry. Geochim Cosmochim Acta 57:2725–2736.

Whittaker RH. 1954. The ecology of serpentine soils. Ecology 35:258–288.

Wu LL, Jacobson AD, Chen HC, Hausner M. 2007. Characterization of elemental release during microbe-basalt interactions at T = 28°C. Geochim Cosmochim Acta 71:2224–2239.

Yao MJ, Lian B. 2011. Weathering of the serpentine and olivine by *Aspergillus fumigatus*. Acta Geol Sin 85:1477–1485.

Zakaznova-Herzog V, Nesbitt H, Bancroft G, Tse J. 2008. Characterization of leached layers on olivine and pyroxenes using high-resolution XPS and density functional calculations. Geochim Cosmochim Acta 72:69–86.